International Journal of Environmental and Biological Sciences
ISSN: 3054-3924
https://doi.org/10.63939/f4e8jf34
Copyright © The Author(s)
Vol. 1 , No 4 , October 2026

RESEARCH Open Access

Structure-Based Design and Molecular Docking Analysis of Uridine-Based and Muraymycin C2 Inhibitors Targeting MraY Translocase in Clinical Isolates *Pseudomonas aeruginosa*

Hawraa Natiq Kabroot AL-Fatlawy

Medical Microbiology, College of Medicine, University of Kufa, Najaf, IRAQ.

hawraan.alfatlawy@uokufa.edu.iq , hawraanatiq@gmail.com

https://orcid.org/0000-0003-0293-8759

Abstract

Background: Multidrug resistance (MDR) *Pseudomonas aeruginosa* has become a major clinical problem because of its resistance to a variety of antibiotic classes and the limited number of effective therapy options. **Objectives:** This study was to perform structure-based design, molecular docking and molecular characterization of Uridine-based and Liponucleoside derivatives of essential translocase in MDR *P. aeruginosa* (*MraY*). **Results:** An antimicrobial resistance profile of (44) forty-four isolates of *P. aeruginosa* revealed high levels of resistance to, cefotaxime, amoxicillin-clavulanic acid and trimethoprim-sulfamethoxazole (100%), and 60% of strains were resistant to the carbapenems. All the clinical isolates were positive results in PCR for the presence of *MraY* gene, it conserved a widespread distribution, and therapeutic importance. Cavity detection and virtual screening in five possible binding pockets resulted in Cavity1 (C1) having a volume of 1819 Å3 at the coordinates (-20, -1, 14) being the main catalytic active site. The natural reference inhibitor Muraymycin C2 showed a high binding interaction of -9.6 kcal/mol within the C1, with significant interactions with the residue ASP115, ASP116, SER120 and THR73. While, the candidate ligand, Uridine 5'-monophosphate, showed a stable and consistent binding score of (-7.6 kcal /mol) in C1, with supporting hydrogen bonds with ALA56, ASP116 and THR71. ADMET and toxicological profiling indicated that Uridine 5'-monophosphate possesses a favorable molecular weight (324.18 g/mol) and compliance with drug-like properties, while both evaluated ligands exhibited exceptionally clean safety profiles, showing no mutagenicity (AMES), hepatotoxicity, cardiotoxicity (hERG) or skin sensitization risks.

Creative Commons Attribution-Non-Commercial 4.0 International License

Published by DAC Democratic Arabic Center
DAC Democratic Arabic Center GmbH, Berlin

Conclusions: The findings highlight that while Muraymycin C2 serves as a high-affinity natural benchmark, the uridine-based scaffold provides a non-toxic and chemically tractable framework for future lead optimization against MDR *P. aeruginosa*.

Keywords: Uridine 5'-monophosphate, MraY translocase, Clinical isolates Multidrug-resistant *Pseudomonas aeruginosa,* ADMET profiling, Muraymycin C2, Structural-based drug design, Molecular docking.

1.Introduction

Pseudomonas aeruginosa is the most clinical pathogen relevant opportunistic pathogens with regards to hospital acquired infections and patients who are immunocompromised. Multidrug resistant (MDR) strains have become a significant health threat worldwide because of the need to develop new antibiotics and the growing ability to develop resistance to these drugs [1-2]. The most important mechanisms that have been identified in *P. aeruginosa* responsible for antimicrobial resistance include target modification, enzymatic inactivation of drugs and decreased overexpression of multidrug efflux pumps and outer membrane permeability [3,4]. Consequently, to identify new and essential targets in bacteria which are not subject to current resistances has become a high priority for antibacterial drug discovery. MraY (Phospho-N-acetylmuramoyl-pentapeptide-transferase) is enzyme in the bacterial cell wall biosynthesis, which is unexploited in clinical applications and thus makes it an attractive target for research of new therapeutic agents. MraY, in particular, facilitates the transfer of phospho-MuNAc-pentapeptide from the cytoplasmic precursor, UDP- MuNAc-pentapeptide, to the lipid carrier undecaprenyl phosphate to form Lipid I, which is a rate limiting step in the peptidoglycan assembly and bacterial survival [5,6]. The MraY inhibition results in cell wall disruption and leads to the rapid bacteriolysis, which makes uridine-based and Liponucleoside scaffolds interesting candidates for overcoming multidrug resistant phenotypes.

Increased resistance to antibiotics has led to the use of computer-aided drug design (CADD) in the discovery of new antibiotic agents. In silico molecular docking technique has emerged as one of the most popular methods for estimating protein-ligand interactions and binding affinity and for the prediction of potential inhibitors before experimental studies [3,7].

Creative Commons Attribution-Non-Commercial 4.0 International License

Published by DAC Democratic Arabic Center
DAC Democratic Arabic Center GmbH, Berlin

In recent years, uridine-based compounds and natural Liponucleoside derivatives have gained great interest as potential antibacterial agents, because of their structural similarity with the natural substrates of bacteria and their high enzyme inhibitory activity [8]. The liponucleoside antibiotics, especially Muraymycin, have been widely documented with high antibacterial activity through competitive inhibition of MraY translocase and disruption of peptidoglycan biosynthesis and the simplified uridine-derived scaffolds provide chemically tractable frameworks with good physiochemical properties for additional medicinal chemistry optimization [9]. Toxicity (ADMET) properties, distribution, prediction of absorption, metabolism and excretion, which are considered an integral part of in silico approaches to drug discovery, has gained increasing importance in early drug discovery to enhance candidate selection and the chances of clinical success. The information obtained from drug-likeness evaluation using Lipinski's rule of five, bioavailability, gastrointestinal absorption and toxicity prediction can prove to be invaluable in pharmacologically determining the suitability of the candidate compounds prior to experimental studies [10].

The aim of the present study was to find and assess potential inhibitors targeting MraY of *P. aeruginosa* by an integrated computational approach. For this, validation and protein preparation, molecular docking of candidate and reference ligands, protein-ligand interaction analysis, as well as ADMET and toxicity prediction of the most promising complex. The results of this study could be used in the identification of novel antibacterial agents (new candidates) that could be effective in combating the multidrug resistant *P. aeruginosa*.

2. Methods and materials

2.1 Clinical isolates and Bacterial Identification

All a total of clinical specimens (613 specimen) from patients suspected to have had a bacterial infection were taken, such as from sputum, urine, wounds and burn samples. Forty-four clinical isolates of Pseudomonas aeruginosa were obtained from various clinical specimens from in-patients. Conventional microbiological and biochemical methods were used for the initial identification; the final identification was done according to the standard working procedures in the laboratory. Multidrug resistance profiles were determined using antimicrobial susceptibility testing, using the method outlined in the CLSI [11].

Creative Commons Attribution-Non-Commercial 4.0 International License

Published by DAC Democratic Arabic Center
DAC Democratic Arabic Center GmbH, Berlin

2.2 Molecular Detection of MraY Target Gene

Bacterial DNA extraction kit was used for genomic DNA extraction following the manufacturer's instructions. The specific primers were used for amplification of the MraY gene by PCR. The MraY gene forward primer F: 5- GTCCGGTCAGCTTGAAGGAA-3' and the reverse primer R: 5- TACATGATGCCGAAACCCC -3' with an amplicon size of 502 bp. The product of the PCR amplification was under an annealing temperature of 59°C for 45sec.

2.3 Phylogenetic and Sequence Analysis of MraY Gene

The nucleotide sequences obtained were analyzed for identity and similarity in the (BLAST) tool available at the NCBI database using the MraY Target gene. The genetic relationship between *P. aeruginosa* isolates and the NCBI reference strains was determined by sequence alignment and phylogenetic analysis using a Tree built by the Fast Minimum Evolution method, available at NCBI.

2.4 Modeling and Validation of MraY Protein

The NCBI ORF Finder was used to obtain protein sequences. The SWISS-MODEL server was used to generate 3-D structures of MraY protein. MolProbity analysis was conducted for structural quality assessment and stereochemical validation, which comprised of Ramachandran plot analysis, side-chain geometry analysis and clash score [12].

2.5 Preparation and Ligand Selection

The candidate and reference ligands were chosen based on prior reports of their antibacterial and inhibitory activities. MraY was used Muraymycin C2 as reference inhibitor and the compound Uridine 5'-monophosphate as candidate ligand. The three-dimensional structures of the ligands were downloaded from the PubChem database and then prepared for suitable docking format using DSV software [13].

Creative Commons Attribution-Non-Commercial 4.0 International License

Published by DAC Democratic Arabic Center
DAC Democratic Arabic Center GmbH, Berlin

2.6 Molecular Docking Analysis to MraY Target

The molecular docking analysis was done using AutoDock Vina embedded in CurPocket to test the binding affinity of the ligands to the MraY target protein. MraY protein preparation involved removal of water molecules, addition of hydrogen atoms and optimization of docking structures. The energy of binding was calculated for every docking pose and the pose with the lowest binding energy was used for further analysis. The interactions of protein-ligand complexes were displayed with Discovery Studio Visualizer [14,15].

2.7 Toxicity Prediction and ADMET Properties

SwissADME web server was used to assess ADMET properties, toxicity and drug-likeness properties of the candidate ligands. The AMES toxicity, hepatotoxicity, hERG inhibition and skin sensitization were predicted using the pkCSM online platform. Also analyzed were Lipinski's rule of five, bioavailability and gastrointestinal absorption parameters [16,17].

2.8 Statistical Analysis

The data was analyzed statistically with SPSS software version 26 and Microsoft Excel [18]. Data were presented in descriptive statistics in the form of frequencies and percentages. Multidrug resistance among clinical isolates of Pseudomonas aeruginosa was compared with the Chi-square (x2) test for the distribution and prevalence of resistance determinants [19].

2.9 Ethical Approval

The study was performed in compliance with ethical principles of the Declaration of Helsinki. All procedures carried out on clinical samples were done in accordance with the patient confidentiality and the institutional ethical guidelines were maintained throughout the study.

Creative Commons Attribution-Non-Commercial 4.0 International License

Published by DAC Democratic Arabic Center
DAC Democratic Arabic Center GmbH, Berlin

3. Results

3.1 Identification and Clinical Characteristics of *Pseudomonas aeruginosa* isolates

The clinical specimens were from patients with bacterial infections and included sputum, urine, wound swabs and burn samples, and covered a wide spectrum of clinical infection sites with a total of 613 specimens. After primary culturing and initial phenotypic screening, (44) isolates were found to be Pseudomonas aeruginosa (7.2%). P. aeruginosa was presumptively identified by characteristic colony morphology, Gram staining properties and pigmentation, which are typical of Gram-negative non-fermentative bacilli. Species-level confirmation was obtained, and there was complete concordance between the phenotypical and the ®VITEK@ND automated identification system. These isolates were clinically proven isolates that were chosen for further antimicrobial susceptibility patterns testing, molecular detection of MraY gene and further in silico analyses. Overall, 44 (7.2%) were positive for P. aeruginosa. Urine accounted for the most specimens (n=342, 55.8%, 23 isolates, 6.7%), followed by sputum (n=130, 21.2%; 12 isolates, highest 9.2%), burns (n=76, 12.4% isolates, 5.3%) and wounds (n=65, 10.6%, 5 isolates, 7.7%).

3.2 Antimicrobial Susceptibility Patterns of *Pseudomonas aeruginosa*

A total of forty-four (44) clinical isolates of *Pseudomonas aeruginosa* were isolated, and their susceptibility patterns were found to have a significantly high proportion of antimicrobial resistance in multiple classes of antibiotics such as β-lactam/β-lactamase inhibitor combinations, aminoglycosides, fluoroquinolones, carbapenems, cephalosporins and folate pathway inhibitors. All isolates (44/44, 100%) were found to be resistant to cefotaxime, amoxicillin-clavulanic acid and trimethoprim-sulfamethoxazole, giving the highest resistance rates. Likewise, ticarcillin-clavulanic acid had a high rate of resistance (43/44, 97.72%). The resistance rate of the aminoglycosides was the highest, with 88.63% (39/44) resistance for amikacin. Imipenem and meropenem resistance were also high (60% or 26/44). Comparatively, low resistance levels were observed against the fluoroquinolone's ciprofloxacin and levofloxacin, 52.27% (23/44) were resistant to each of these.

Creative Commons Attribution-Non-Commercial 4.0 International License

Published by DAC Democratic Arabic Center
DAC Democratic Arabic Center GmbH, Berlin

The results showed significant antimicrobial resistance distribution among the isolates studied, indicating that they are less susceptible to various antimicrobial classes. The above results indicate that there is considerable burden of multidrug resistance (MDR) in the study population. However, classification of individual isolates as MDR or extensively drug-resistant (XDR) depends on the susceptibility results to the specified categories of antimicrobial drugs and the use of the internationally accepted definitions.

3.3 Molecular Detection and Sequence Confirmation of Target Gene

MraY (phospho-N-acetylmuramoyl-pentapeptide-transferase) gene was revealed in all 44(100%) clinical strains of *P. aeruginosa*, hence it was universally present in all the *P. aeruginosa* strains examined. The regularity of the detection of these target gene in all of the isolates reinforces the relevance of this gene in the bacterial viability and confirms their choice to be targeted by further molecular and in-silico studies. The representative PCR amplification profiles of the *MraY* gene IS are presented in Figure 1. A representative set of PCR positive isolates was used for sequence analysis, and 4 isolate for *MraY* at sequence level characterization. Sequencing of DNA was done. To verify the identities of the obtained sequences and sequence similarity before multiple sequence alignment, mutation assessment and modeling of protein structure, the sequences were analyzed by BLAST algorithm at National Center for Biotechnology Information (NCBI).

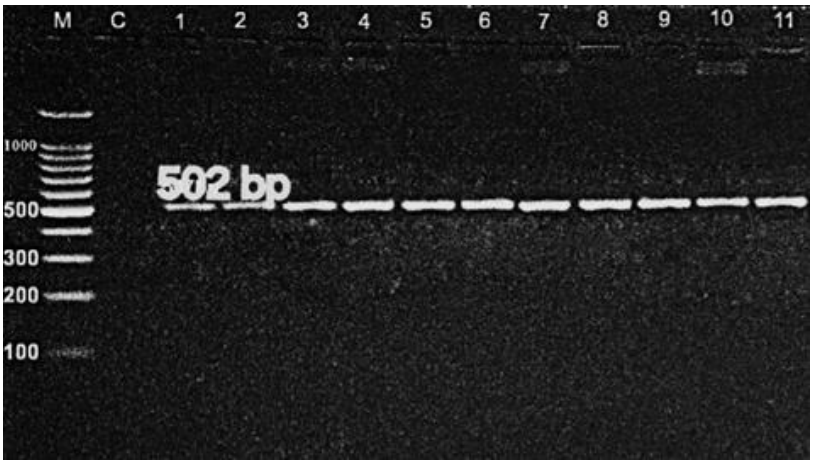


Figure 1. PCR amplification results of The *MraY* Target gene in MDR *Pseudomonas aeruginosa*. Demonstrating a specific amplicon at the expected size 502 bp.
M: DNA Molecular (DNA ladder) and lanes 1- 11: positive isolates for *MraY* gene.

Creative Commons Attribution-Non-Commercial 4.0 International License

Published by DAC Democratic Arabic Center
DAC Democratic Arabic Center GmbH, Berlin

3.4 Genetic Variability and Sequence Analysis of MraY target

Sequence characterization of the *MraY* gene indicated substantial genetic similarity to previously reported *Pseudomonas aeruginosa* sequences available in the NCBI database. The results of BLAST alignment revealed sequence identity values ranging from approximately 95% to 99%, indicating a high level of conservation of the *MraY* gene among the investigated clinical isolates. Furthermore, analysis of the deduced MraY protein sequence identified conserved regions associated with its function in peptidoglycan biosynthesis. The preservation of these functional domains highlights the potential importance of MraY as a promising target for the development of alternative antibacterial agents.

The phylogenetic tree further supported these findings, as the examined clinical isolates exhibited close evolutionary relationships with the corresponding reference strains, reflecting the genetic relatedness and conservation of the MraY gene (Figure 2).

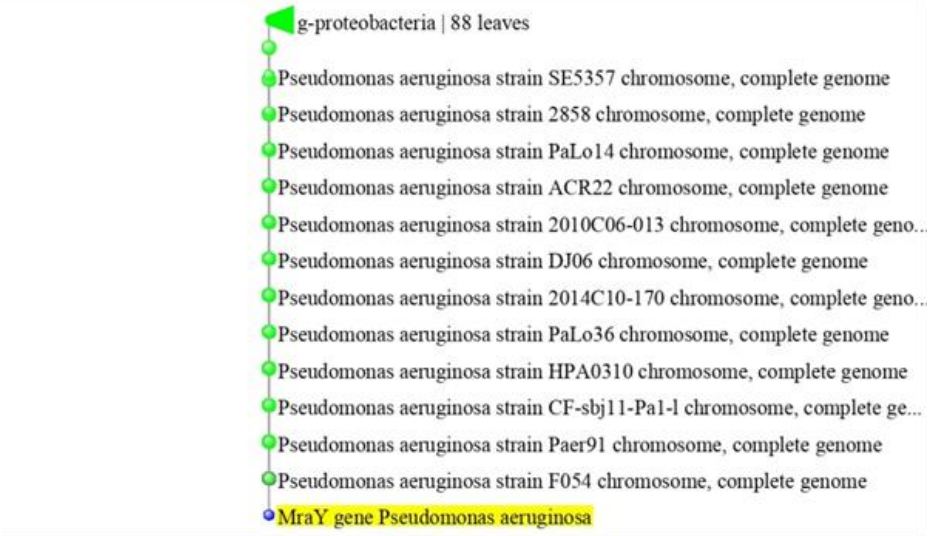


Figure 2. The Phylogenetic tree of the *MraY* gene among Pseudomonas aeruginosa. Phylogenetic tree was constructed using *MraY* nucleotide sequences retrieved from the NCBI database, showing the genetic relationships between the investigated clinical isolates

Creative Commons Attribution-Non-Commercial 4.0 International License

Published by DAC Democratic Arabic Center
DAC Democratic Arabic Center GmbH, Berlin

and reference strains. Tree construction was performed using the Fast Minimum Evolution Method.

3.5 Preparation, Modeling and Validation of MraY Target Protein

The 3D dimensional structure of the MraY target protein. *MraY* was generated and prepared for subsequent molecular docking investigations. Initially, the nucleotide sequence *MraY* gene was retrieved from the NCBI database, followed by translation into its corresponding amino acid sequence according to the predicted open reading frame (ORF). The resulting protein sequence was then utilized as input for three-dimensional structural prediction.

Protein homology modeling was carried out using the SWISS-MODEL online platform. Appropriate structural templates exhibiting high sequence similarity and extensive coverage were selected to generate the predicted protein model. The quality of the resulting structure was assessed using different evaluation parameters to establish its suitability for molecular docking studies. The obtained MraY model exhibited a Global Model Quality Estimation (GMQE) score 0.93, with 61% sequence identity and coverage spanning amino acid residues 1-360. Furthermore, the predicted structure contained transmembrane regions, which are consistent with the membrane-associated nature of MraY and involvement in bacterial peptidoglycan synthesis.

Prior to docking analysis, protein preparation involved the incorporation of hydrogen atoms and structural refinement through energy minimization to improve the stability of the generated model. Potential ligand-binding regions were identified with particular attention to conserved functional domains, including the ATP-binding pocked and the catalytic residues of MraY. The predicted three-dimensional structure of MraY protein is illustrated in Figure 3.

Creative Commons Attribution-Non-Commercial 4.0 International License

Published by DAC Democratic Arabic Center
DAC Democratic Arabic Center GmbH, Berlin

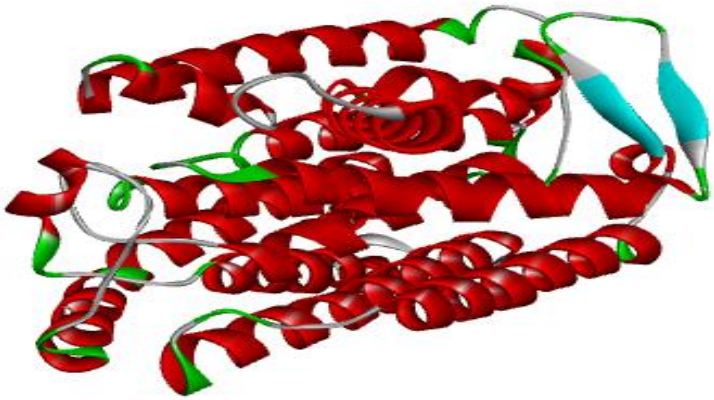


Figure 3. Three-dimensional homology model and structural validation of MraY protein.

The predicted three-dimensional structure of MraY was constructed using the SWISS-MODEL server, followed by structural assessment through MolProbity analysis. The resulting model represents the predicated conformation and structure quality of the target protein. Following refinement and validation, the optimized MraY structure was employed in subsequent molecular docking studies.

3.6 ADMET Profiling of Muraymycin C2 and Uridine Inhibitor

A total of two compounds were selected for Molecular docking analysis against the MraY protein, comprising a reference inhibitor and a potential candidate ligand. Muraymycin C2 was included as a reference compound due to its reported inhibitory activity against MraY providing a comparative standard for evaluating ligand-protein interactions. In addition, Uridine 5'-monophosphate (UMP) was selected as a candidate ligand based on its structural relationship to nucleotide-derived substrates involved in the biological function of MraY and its potential to interact with conserved regions of the target protein.

The chemical structures of both compounds were retrieved from public chemical databases and subjected to ligand preparation, including geometry optimization and energy minimization, before molecular docking. Furthermore, their physicochemical characteristics and predicted pharmacokinetic properties were evaluated using in silico

Creative Commons Attribution-Non-Commercial 4.0 International License

Published by DAC Democratic Arabic Center
DAC Democratic Arabic Center GmbH, Berlin

ADMET analysis, considering Lipinski's Rule of Five, gastrointestinal absorption and potential toxicity. The selected compounds and their classifications in Table 1.

Table 1. Reference inhibitor and candidate ligand selected for molecular docking and in silico ADMET evaluation against the MraY Protein.

Target protein	Reference inhibitor	Candidate inhibitors	Chemical /Functional class
MraY	**Muraymycin C2**	**Uridine 5' monophosphate (Candidate)**	Peptidoglycan biosynthesis inhibitor

3.7 Molecular Docking Analysis of the Selected Ligands

3.7.1. Binding Site Identification and Binding Cavity Analysis of MraY protein

To determine the most favorable catalytic pocket for inhibiting the MraY translocase in multidrug-resistant (MDR) *Pseudomonas aeruginosa*, virtual screening and cavity detection were conducted across five potential binding pockets (C1 to C5). The spatial dimensions and grid coordinates of each evaluated cavity, along with their respective binding energy profiles are detailed in (Table 2), Among the detected binding cavity, Cavity1 (C1) demonstrated the highest structural capacity, displaying a total cavity volume of 1819 $Å^3$ centered at coordinates (x:-20, y:-1, z:14). The substantial volumetric capacity of C1 provided an optimal microenvironment for accommodating the uridine-based ligand framework without incurring unfavorable steric clashes.

3.7.2 Molecular Docking Analysis of Uridine 5- Monophosphate (UMP) Against MraY Binding Cavities

Molecular docking assessment of Uridine 5-monophosphate (UMP) against the predicted binding cavities of the MraY protein revealed Vina affinity scores ranging from -5.3 to -7.6 kcal/mol (Table.2). Variations in docking scores among the identified cavities suggest differences in their ligands-binding potential

Primary Binding Cavity (C1): Among the analyzed binding sites, cavity C1 demonstrated the most favorable docking score, reaching -7.6 kcal/mol, with a calculated volume of 1819

Creative Commons Attribution-Non-Commercial 4.0 International License

Published by DAC Democratic Arabic Center
DAC Democratic Arabic Center GmbH, Berlin

Å^3. This result indicates a comparatively favorable predicted interaction between UMP and this binding region. The relatively large dimensions of C1 may provide sufficient space to accommodate the ligand and facilitate multiple intermolecular contacts, potentially involving hydrogen bonding and other non-covalent interactions with amino acid residues lining the cavity.

Secondary Binding Cavities (C2-C5): Cavity C2 exhibited the second-best predicted binding affinity, with a Vina score of -6.9 kcal/mol and a volume of 390 Å^3. In comparison cavities C3, C4 and C5 showed less favorable docking scores, with a reported value of approximately - 5.6 kcal/mol, and cavity volumes of 313, 236 and 175 Å^3, respectively. Overall, cavity C1 exhibited the most favorable docking result among the investigated binding regions, suggesting that it may represent a potential ligand-binding site for UMP within the MraY protein of *Pseudomonas aeruginosa*. Nevertheless, further examination of ligand-protein interactions and experimental validation are necessary to establish its functional relevance and determine whether UMP can interfere with MraY enzymatic activity.

Table 2. Docking scores, cavity dimensions, and grid parameters of Uridine 5'-monophosphate within the predicted binding pockets of MraY translocase.

Cavity ID	Vina score (kcal/mol)	Volume (Å^3)	Center (x, y, z)	Docking size (x, y, z)
C1	-7.6	1819	-20, -1, 14	19, 19, 19
C2	-6.9	390	-13, 8, -10	19, 19, 19
C5	-5.6	175	-28, 7, 2	19, 19, 19
C3	-5.5	313	-2, 0, 17	19, 19, 19
C4	-5.3	236	-22, -10, 10	19, 19, 19

Creative Commons Attribution-Non-Commercial 4.0 International License

Published by DAC Democratic Arabic Center
DAC Democratic Arabic Center GmbH, Berlin

3.7.3 Molecular Interactions Analysis of MraY-UMP Complex in Binding Cavity C1

Binding interactions within MraY-UMP complex Cavity C1 illustrated in (Figure 4 A, B and Table 4) revealed a robust and network of non-covalent interactions that secure the Uridine 5'-monophosphate ligand within the active site of the MraY translocase (Chain A):

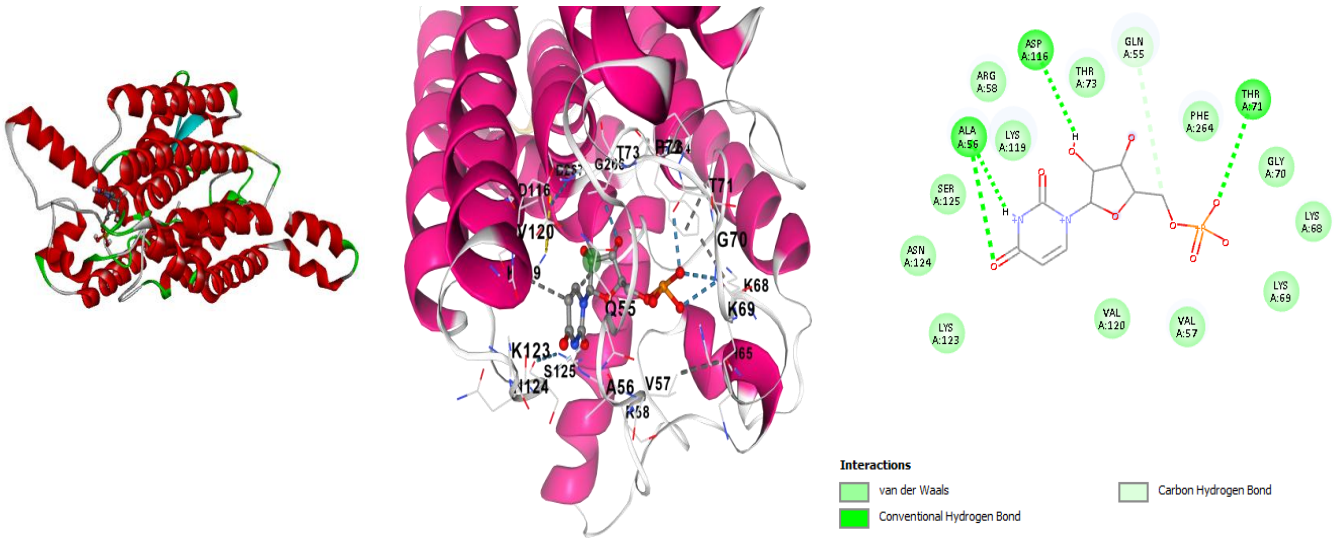
Hydrogen bonding and electrostatic interactions: Conventional hydrogen bonds are prominently formed with key catalytic residues, notably ASP116 (interacting with the ribose hydroxyl group), ALA56 (interacting with the uracil ring backbone) and THR71 (stabilizing the phosphate moiety). These directional bonds significantly contribute to the superior binding affinity (-7.6 kcal/mol).

Carbon –hydrogen bonds and Van der Waals contacts: Additional stability is mediated via extensive van der Waals and carbon-hydrogen interactions involving surrounding residues within the pocket, including GLN52 GLN55 ALA56 VAL57 ARG58 HIS65 LEU66 LYS68 LYS69 GLY70 THR71 PRO72 THR73 MET74 ASP116 LYS119 VAL120 LYS123 ASN124 SER125 ASN192 ASP195 GLY196 LEU197 PHE264 MET265 GLY266 ASP267 HIS326.

The convergence of high volumetric capacity favorable thermodynamic score and a robust hydrogen bonding network confirms that Cavity C1 is the authentic primary active site, providing a solid structural foundation for designing advanced uridine-based translocase inhibitors against MDR *Pseudomonas aeruginosa.*

Creative Commons Attribution-Non-Commercial 4.0 International License

Published by DAC Democratic Arabic Center
DAC Democratic Arabic Center GmbH, Berlin



(A) **(B)**

Figure 4 (A,B). Structural visualization and interaction profile of the MraY-Uridine 5'-monophosphate (UMP) Complex. (A): Three-dimensional representation of UMP docked within the binding cavity MraY protein. **(B):** Detailed illustration of the intermolecular interactions between UMP and the surrounding amino acid residues, highlighting hydrogen bonds, π-interactions and hydrophobic contacts within the binding pocket.

3.7.4. Molecular Docking and Interaction Profile of Muraymycin C2 Inhibitor

Molecular docking simulation were performed using the natural Liponucleoside antibiotic Muraymycin C2, to validate the structural reliability of the MraY translocase active site (Cavity C1) and establish a comparative benchmark. Muraymycin C2 demonstrated an exceptionally high binding affinity within Cavity C1, achieving a prominent Vina docking score of -9.6 kcal/mol (Table.3).

When compared to the Uridine 5'monophosphate core (-7.6 kcal/mol), Muraymycin C2 exhibited a significantly enhanced negative binding energy (ΔΔG=-2.0 kcal/mol). This pronounced energetic superiority underscores the critical biological role of the integrated peptide and lipid-like side chains native to Liponucleoside inhibitors, which allow optimal hydrophobic and electrostatic integration within the extended translocase binding channel

Creative Commons Attribution-Non-Commercial 4.0 International License

Published by DAC Democratic Arabic Center
DAC Democratic Arabic Center GmbH, Berlin

of *Pseudomonas aeruginosa* MraY. Alternative cavities (C5, C2, C4 and C3) yielded considerably lower binding scores of -8.4, -6.8, -6.4 and -5.2 kcal/mol, respectively, further confirming that Cavity C1 serves as the primary catalytic site for both natural Liponucleoside inhibitors and uridine-based scaffolds.

Table.3: Molecular Docking scores, binding cavity volumes and grid parameters of Muraymycin C2 within the predicted binding pockets of MraY translocase

Cavity ID	Vina score (kcal/mol)	Volume (Å^3)	Center (x, y, z)	Docking size (x, y, z)
C1	-9.6	1819	-20, -1, 14	28, 28, 28
C5	-8.4	175	-28, 7, 2	28, 28, 28
C2	-6.8	390	-13, 8, -10	28, 28, 28
C4	-6.4	236	-22, -10, 10	28, 28, 28
C3	-5.2	313	-2, 0, 17	28, 28, 28

3.7.5. Protein-Ligand Interaction Network in Cavity C1 of Muraymycin C2

Dimensional interaction analysis (illustrated in Figure,5: A-B and Table.4) revealed an extensive multi-anchored non-covalent bonding network that stabilizes Muraymycin C2 within Cavity C1 (Chain A):

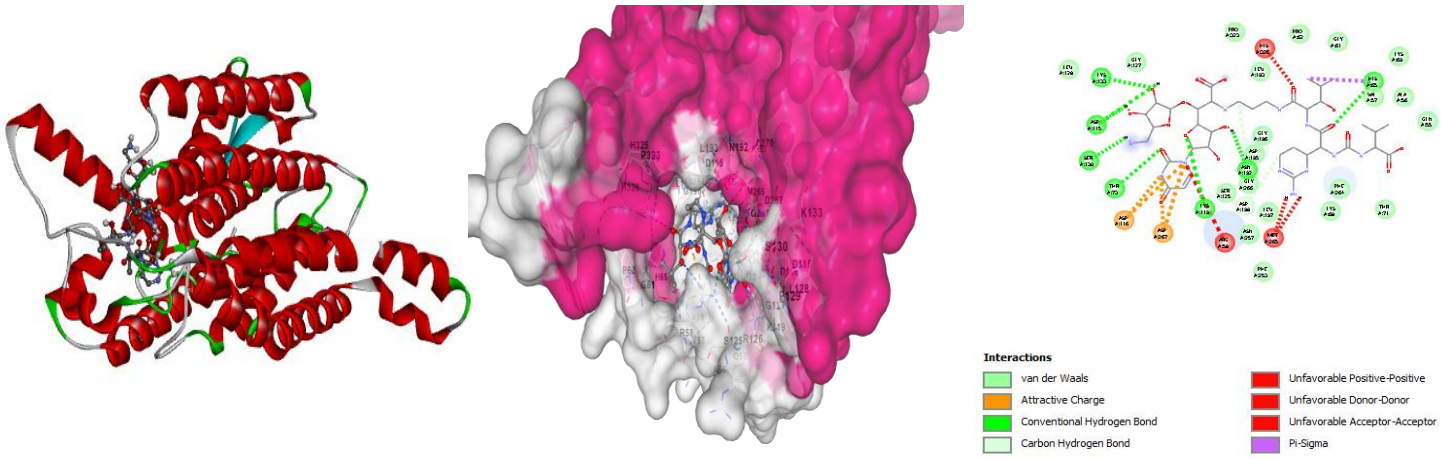
Hydrogen Bonding and Electrostatic Stabilizations: conventional hydrogen bonds and attractive charge interactions heavily anchor the complex. Key catalytic residues actively participating include ASP115, ASP116, SER120, THR73, GLY127, LYS123, ASP267, and MET265, forming strong directional bonds with the nucleoside and peptide moieties of Muraymycin C2.

Hydrophobic and Pi-interactions: The complex is further reinforced by extensive van der Waals contacts and hydrophobic interactions across a broad spectrum of surrounding residues, including GLN55 ALA56 VAL57 ARG58 ASP60 GLY61 PRO62 HIS65 LEU66

Creative Commons Attribution-Non-Commercial 4.0 International License

Published by DAC Democratic Arabic Center
DAC Democratic Arabic Center GmbH, Berlin

LYS68 LYS69 GLY70 THR71 PRO72 THR73 ASP115 ASP116 LYS119 VAL120 LYS123 ASN124 SER125 ARG126 GLY127 LEU128 PRO129 SER130 LYS133 GLN137 ASN189 VAL191 ASN192 LEU193 THR194 ASP195 GLY196 LEU197 ASP198 PHE253 ASN257 VAL263 PHE264 MET265 GLY266 ASP267 ALA270 LEU271 VAL304 GLN307 VAL308 ARG317 MET321 ALA322 PRO323 HIS325 HIS326 GLU335



(A) **(B)**

Figure 5 (A, B). Structural representation and intermolecular interaction analysis of the MraY-Muraymycin C2 complex within binding cavity C1. (A): Three-dimensional visualization of Muraymycin C2 accommodated within the C1 binding cavity of the MraY protein. **(B):** Detailed representation of the interactions between Muraymycin C2 and the surrounding amino acid residues, illustrating hydrogen bonds, π-interactions, and hydrophobic contacts involved in ligand stabilization within the binding pocket.

Table.4 . Summary of Key Amino Acid Residues and Intermolecular Interactions in MraY-ligand Complexes

Target protein	Ligand	Interaction type	Hydrogen – bonds interactions	II-interactions	Hydrophobic contacts	Key interacting Residues
MraY	Muraymycin C2	Reference	ASP115, ASP116, SER120, THR73,	His65 (Pi-sigma)	GLN55 ALA56 VAL57 ARG58	ARG58 ASP116 LYS123, ASP267

Creative Commons Attribution-Non-Commercial 4.0 International License

Published by DAC Democratic Arabic Center
DAC Democratic Arabic Center GmbH, Berlin

			GLY127, LYS123, ASP267, MET265		ASP60 GLY61 PRO62 HIS65 LEU66 LYS68 LYS69 GLY70 THR71 PRO72 THR73 ASP115 ASP116 LYS119 VAL120 LYS123 ASN124 SER125 ARG126 GLY127 LEU128 PRO129 SER130 LYS133 GLN137 ASN189 VAL191 ASN192 LEU193 THR194 ASP195 GLY196 LEU197 ASP198 PHE253 ASN257 VAL263 PHE264 MET265 GLY266 ASP267 ALA270	

Creative Commons Attribution-Non-Commercial 4.0 International License

Published by DAC Democratic Arabic Center
DAC Democratic Arabic Center GmbH, Berlin

					LEU271 VAL304 GLN307 VAL308 ARG317 MET321 ALA322 PRO323 HIS325 HIS326 GLU335	
MraY	Uridine 5'-monophosphate	Candidate	ALA56 ASP116 THR71	-	GLN52 GLN55 ALA56 VAL57 ARG58 HIS65 LEU66 LYS68 LYS69 GLY70 THR71 PRO72 THR73 MET74 ASP116 LYS119 VAL120 LYS123 ASN124 SER125 ASN192 ASP195 GLY196 LEU197 PHE264 MET265 GLY266 ASP267 HIS326	ALA56 ASP116 THR71 LYS69

Creative Commons Attribution-Non-Commercial 4.0 International License

Published by DAC Democratic Arabic Center
DAC Democratic Arabic Center GmbH, Berlin

The comparative interaction profiling within the primary catalytic cavity (C1) of *Pseudomonas aeruginosa* MraY demonstrates distinct binding behaviors between the candidate uridine derivative and the natural reference inhibitor. Uridine 5'-monophosphate anchors primarily through key hydrogen bonds involving ALA56, ASP116 and THR71, alongside standard van der Waals contacts. In comparison, the reference inhibitor Muraymycin C2 demonstrated a more extensive interaction profile within the MraY binding cavity, forming multiple hydrogen bonds with several amino acid residues, including ASP115, ASP116, SER120, THR73, GLY127, LYS123, ASP267 and MET265. Additionally, a π-sigma interaction was identified involving HIS65, accompanied by numerous hydrophobic contacts distributed throughout the translocase binding channel. These interaction patterns suggest that the extended peptidyl structure and lipid-associated moieties of Muraymycin C2 may contribute to improved accommodation within the binding pocket and enhanced ligand-protein interactions, potentially supporting greater complex stability and binding affinity.

3.8. ADMET and Toxicity Analysis of Uridine and Muraymycin C2

ADMET and toxicity assessment were conducted for Uridine 5'-monophosphate (UMP), designated as the candidate compound, and Muraymycin C2 used as the reference control, to investigate their predicted pharmacokinetic characteristics and potential safety profiles.

Absorption and Pharmacokinetics Properties: Both compounds were predicted to exhibit low gastrointestinal (GI) absorption through passive transmembrane transport, indicating that their systemic bioavailability may be limited. Accordingly, formulation-based approaches, targeted delivery systems or prodrug strategies may be required to improve their absorption and facilitate systemic administration.

Biosafety and Toxicological Assessment: Notably, the silico predictions indicated favorable safety profiles for both compounds, with no major toxicity alerts identified in the evaluated parameters. Neither compound presented mutagenic risks (**AMES: No**),

Creative Commons Attribution-Non-Commercial 4.0 International License

Published by DAC Democratic Arabic Center
DAC Democratic Arabic Center GmbH, Berlin

hepatotoxicity (**Hepatotoxicity: No**), cardiotoxicity liabilities (**hERG I/II: No/No**), or contact dermal allergies (**Skin Sensitisation**: No).

Overall, while Muraymycin C2 achieves higher binding energy due to its extended lipopeptidic architecture, Uridine 5'-monophosphate provides a superior, non-toxic and chemically tractable scaffold for lead optimization against multidrug-resistant *Pseudomonas aeruginosa* (Table.5).

Table.5: In silico evaluation of ADMET, drug-likeness and toxicity profiling of the candidate uridine derivative in comparison with the reference inhibitor**.**

Tested compound (Ligand)	Molecular mass ,MW (g/mol)	Polar Surface area TPSA ,Å^2)	Intestinal Absorption (GI)	Drug-likeness assessment	Bioavailability	AMES	Hepatotoxicity	hERG I/II	Skin Senstisation
Uridine 5' monophosphate (Candidate)	324.18	181.12	low	No (1 violation: NorO>10)	0.11	No	No	No/No	No
Muraymycin C2 Reference	931.94	446.09	low	No (3 violations)	0.17	No	No	No/No	No

4. Discussion

The emergence and widespread dissemination of multidrug-resistant *Pseudomonas aeruginosa* have substantially complicated antimicrobial treatment, largely owing to the bacterium's capacity to develop and utilize diverse resistance strategies, including alterations in antimicrobial targets and the activation of multidrug efflux systems. In the current investigation, molecular analysis revealed the presence of *MraY* gene among the examined bacterial isolates, highlighting its relevance as a potential molecular target in the investigation of bacterial resistance and survival. These observations are consistent with previous reports emphasizing the biological significance of MraY in bacterial cell viability and its potential relevance to antimicrobial target development [20,21].

Assessment of the predicted MraY protein structure revealed satisfactory stereochemical characteristics, as supported by MolProbity scores and Ramachandran plot

Creative Commons Attribution-Non-Commercial 4.0 International License

Published by DAC Democratic Arabic Center
DAC Democratic Arabic Center GmbH, Berlin

analysis. Such validation procedures are important for establishing the structural reliability of computationally generated protein models, particularly when these structures are subsequently employed in molecular docking. Comparable structural modeling and validation strategies have been adopted in earlier computational investigations of bacterial proteins associated with antimicrobial resistance [22,23].

Inhibition of bacterial cell wall formation constitutes a well-established approach in antibacterial drug development. Among the potential molecular targets, phospho-N-acetylmuramoyl-pentapeptide-transferase (MraY) has attracted considerable attention because of its essential function in the biosynthesis of Lipid I, a key intermediate in peptidoglycan assembly. Its essential biological role makes MraY an attractive candidate for the development of novel antibacterial agents, particularly against multidrug-resistant Pseudomonas aeruginosa [24].

In this context, the present investigation employed structural cavity analysis and molecular docking approaches to characterize the potential binding interactions of uridine 5'-monophosphate (UMP), the selected candidate ligand, in comparison with Muraymycin C2, a naturally occurring liponucleoside inhibitor. This computational analysis provided insights into the predicted ligand-binding modes and the molecular interactions potentially contributing to ligand recognition within the MraY binding pocket.

Structural cavity mapping revealed that Cavity C1, with an estimated volume of 1,819 $Å^3$ represents the most prominent binding region with the *P. aeruginosa* MraY structure. The considerable dimensions of this cavity may provide sufficient spatial accommodation for the native substrate, UDP-MurNAc-pentapeptide, and its associated lipid carries, undecaprenyl phosphate during the enzymatic process. Both investigated compounds exhibited a preferential binding orientation within Cavity C1 compared with the other identified cavities (C2-C5), confirming that this region constitutes the principal ligand-binding site in the predicted protein structure.

Comparative of the docking-derived binding energies demonstrated a difference in the predicted affinity between the reference inhibitor, Muraymycin C2 (-9.6 kcal/mol), and the candidate compound, uridine 5'-monophosphate (-7.6 kcal/mol). The more favorable energy value obtain for Muraymycin C2 indicates stronger predicted binding within the

Creative Commons Attribution-Non-Commercial 4.0 International License

Published by DAC Democratic Arabic Center
DAC Democratic Arabic Center GmbH, Berlin

MraY binding pocket relative to UMP. Nevertheless, the binding energy estimated for UMP suggests a potentially favorable interaction with the target protein. This energy differential ΔΔG= -2.0 kcal/mol) reflects the structural complexity of Muraymycin C2, whose extended peptide and lipophilic side chains establish a multi-anchored network across the transmembrane groove, including conventional hydrogen bonds (notably with ASP115, ASP116, SER120, THR73, GLY127, LYS123, ASP267 and MET265) and a stabilizing Pi-sigma interaction with HIS65. These finding align with recent structural and biochemical breakthroughs demonstrating that the Lipopeptidic tail of Muraymycin mimics the native lipid carrier, occupying hydrophobic sub-pockets to achieve potent antibacterial inhibition [25].

Conversely, although Uridine 5-monophosphate lacks the lipopeptidic tail, it achieved a highly favorable binding score of (-7.6 kcal/mol) by anchoring directly within the conserved uridine-binding sub-pocket of Cavity C1. Specifically, the formation of directional hydrogen bonds with ALA56, ASP116, and THR71 residues critically involved in coordinating the uracil base, ribose hydroxyls and phosphate moiety demonstrates that the core uridine monophosphate scaffold is sufficient to drive strong, specific recognition by MraY. Notably, ASP116 served as a shared catalytic anchor for both ligands, underscoring its pivotal role in stabilizing nucleoside-based inhibitors with the active site of *P. aeruginosa* MraY.

Integrated of the molecular docking analysis results with the predicted ADMET profiles revealed an important distinction between binding performance and drug-likeness characteristics. Although, Muraymycin C2 exhibits superior binding affinity, its high molecular mass (931.94 g/mol), extensive topological polar surface area (446.09 $Å^2$) and multiple Lipinski violations pose significant synthetic and pharmacokinetic challenges [26,27]. In contrast, Uridine 5'-monophosphate offers a compact (324.18 g/mol), non-toxic and chemically tractable core that retains key catalytic interactions within Cavity C1. Consequently, rational structural modification of this uridine scaffold such as introducing hydrophobic or peptidomimetic linkers to engage adjacent sub-pockets (e.g., HIS65 and LYS123) represents a promising avenue for developing potent drug-like MraY inhibitors against MDR *P. aeruginosa* [28].

Creative Commons Attribution-Non-Commercial 4.0 International License

Published by DAC Democratic Arabic Center
DAC Democratic Arabic Center GmbH, Berlin

Conclusions:

The present study confirms the conserved presence of the MraY gene across 44 multidrug-resistant Pseudomonas aeruginosa clinical isolates, validating MraY translocase as a prime therapeutic target. Structure-based docking identified Cavity C1as the primary active site, where Uridine 5-monophosphate achieved strong binding affinity (-7.6 kcal/mol) via key hydrogen bonds with ASP116, ALA56 and THR71, closely mirroring the core interactions of the natural reference Muraymycin C2 (-9.6 kcal/mol). Combined with its compact molecular weight and clean ADMET safety profile, the uridine-based scaffold represents a safe, chemically tractable lead candidate for future for structural optimization against MDR *P. aeruginosa.*

Highlights

- Conserved MraY gene distribution confirmed across clinical MDR P. aeruginosa isolates.
- Primary catalytic binding pocket identified within the MraY translocase channel.
- Uridine-based candidate anchored firmly via key catalytic hydrogen-bonding residues.
- Muraymycin C2 reference established strong binding through extended lipopeptidic contacts.
- Uridine scaffold showed clean ADMET safety and tractability for anti-MDR lead optimization.

Declarations:

Ethics declaration

This research was conducted in accordance with the ethical principles established by the Declaration of Helsinki. The collection and handling of clinical specimens adhered to the relevant institutional ethical requirements. Throughout the study, strict measures were implemented to safeguard patient privacy and ensure the confidentiality of all clinical information.

Creative Commons Attribution-Non-Commercial 4.0 International License

Published by DAC Democratic Arabic Center
DAC Democratic Arabic Center GmbH, Berlin

Consent to publication: not applicable

Acknowledgment

The author would like to express sincere gratitude to the Faculty of Medicine, University of Kufa, particularly the Postgraduate Molecular Biology Laboratory, Department of Microbiology, for providing the laboratory facilities and research environment that enabled the successful completion of this study.

Author Contributions

Hawraa Natiq Kabroot AL-Fatlawy independently conceived and designed the study, performed all experimental procedures, conducted molecular and bioinformatics analysis, interpreted the data, and drafted and revised the research paper.

Funding: funding is no financial support for publication or the research.

Conflict of Interest

The author declares that there is no conflict of interest, whether financial or personal, that could have influenced the research, or preparation of this manuscript.

References:

1- Avakh, A., Grant, G. D., Cheesman, M. J., Kalkundri, T., & Hall, S. (2023). The Art of War with *Pseudomonas aeruginosa*: Targeting Mex Efflux Pumps Directly to Strategically Enhance Antipseudomonal Drug Efficacy. *Antibiotics (Basel, Switzerland)*, *12*(8), 1304. https://doi.org/10.3390/antibiotics12081304

2- Abdallah, E. M., Alhudhaibi, A. M., Dahab, M., Al Noman, A., Sharma, P. D., Taha, T. H., & Nawaz, M. (2026). The WHO priority list of antibiotic-resistant bacteria: Challenges and opportunities for next-generation antimicrobial development. *Frontiers in Pharmacology*, *17*, 1699987. https://doi.org/10.3389/fphar.2026.1699987

3- Pang, Z., Raudonis, R., Glick, B. R., Lin, T. J., & Cheng, Z. (2019). Antibiotic resistance in Pseudomonas aeruginosa: mechanisms and alternative therapeutic

Creative Commons Attribution-Non-Commercial 4.0 International License

Published by DAC Democratic Arabic Center
DAC Democratic Arabic Center GmbH, Berlin

strategies. *Biotechnology advances*, *37*(1), 177–192. https://doi.org/10.1016/j.biotechadv.2018.11.013

4- Breidenstein, E. B., de la Fuente-Núñez, C., & Hancock, R. E. (2011). Pseudomonas aeruginosa: all roads lead to resistance. *Trends in microbiology*, *19*(8), 419–426. https://doi.org/10.1016/j.tim.2011.04.005

5- Chung, B. C., Zhao, J., Gillespie, R. A., Kwon, D. Y., Guan, Z., Hong, J., Zhou, P., & Lee, S. Y. (2013). Crystal Structure of MraY, an Essential Membrane Enzyme for Bacterial Cell Wall Synthesis. *Science (New York, N.Y.)*, *341*(6149), 1012. https://doi.org/10.1126/science.1236501

6- Mashalidis, E. H., Kaeser, B., Terasawa, Y., Katsuyama, A., Kwon, D. Y., Lee, K., Hong, J., Ichikawa, S., & Lee, S. Y. (2019). Chemical logic of MraY inhibition by antibacterial nucleoside natural products. *Nature Communications*, *10*(1), 2917. https://doi.org/10.1038/s41467-019-10957-9

7- Gervasoni, S.; Malloci, G.; Bosin, A.; Vargiu, A.V.; Zgurskaya, H.I.; Ruggerone, P. Recognition of quinolone antibiotics by the multidrug efflux transporter MexB of Pseudomonas aeruginosa. *Phys. Chem. Chem. Phys.* **2022**, *24*, 16566–16575. DOI: https://doi.org/10.1039/d2cp00951j

8- Phan, T. V., Nguyen, V. T., Le, M. T., Nguyen, B. G. D., Vu, T. T., & Thai, K. M. (2024). Identification of efflux pump inhibitors for Pseudomonas aeruginosa MexAB-OprM via ligand-based pharmacophores, 2D-QSAR, molecular docking, and molecular dynamics approaches. *Molecular diversity*, *28*(5), 3295–3311. https://doi.org/10.1007/s11030-023-10758-9

9- Dey D, Kavanaugh LG, Conn GL2020.Antibiotic Substrate Selectivity of Pseudomonas aeruginosa MexY and MexB Efflux Systems Is Determined by a Goldilocks Affinity. Antimicrob Agents Chemother64:10.1128/aac.00496-20. https://doi.org/10.1128/aac.00496-20

10- Babalola, B. A., Malik, M., Olowokere, O., Adebesin, A., & Sharma, L. (2025). Indoles in drug design and medicinal chemistry. *European Journal of Medicinal Chemistry Reports*, *13*, 100252. https://doi.org/10.1016/j.ejmcr.2025.100252

11- Schuetz, A. N., Ferrell, A., Hindler, J. A., Humphries, R., & Bobenchik, A. M. (2025). Overview of changes in the Clinical and Laboratory Standards Institute

Creative Commons Attribution-Non-Commercial 4.0 International License

Published by DAC Democratic Arabic Center
DAC Democratic Arabic Center GmbH, Berlin

Performance Standards for Antimicrobial Susceptibility Testing: M100 32nd and 33rd editions. *Journal of Clinical Microbiology*, *63*(9), e01623-23. https://doi.org/10.1128/jcm.01623-23

12- Waterhouse, A., Bertoni, M., Bienert, S., Studer, G., Tauriello, G., Gumienny, R., Heer, F. T., de Beer, T. A. P., Rempfer, C., Bordoli, L., Lepore, R., & Schwede, T. (2018). SWISS-MODEL: homology modelling of protein structures and complexes. *Nucleic acids research*, *46*(W1), W296–W303. https://doi.org/10.1093/nar/gky427

13- Kim, S., Chen, J., Cheng, T., Gindulyte, A., He, J., He, S., Li, Q., Shoemaker, B. A., Thiessen, P. A., Yu, B., Zaslavsky, L., Zhang, J., & Bolton, E. E. (2023). PubChem 2023 update. *Nucleic acids research*, *51*(D1), D1373–D1380. https://doi.org/10.1093/nar/gkac956

14- Liu, Y., Yang, X., Gan, J., Chen, S., Xiao, Z. X., & Cao, Y. (2022). CB-Dock2: improved protein-ligand blind docking by integrating cavity detection, docking and homologous template fitting. *Nucleic acids research*, *50*(W1), W159–W164. https://doi.org/10.1093/nar/gkac394

15- Yang, X., Liu, Y., Gan, J., Xiao, Z. X., & Cao, Y. (2022). FitDock: protein-ligand docking by template fitting. *Briefings in bioinformatics*, *23*(3), bbac087. https://doi.org/10.1093/bib/bbac087

16- Daina, A., Michielin, O., & Zoete, V. (2017). SwissADME: A free web tool to evaluate pharmacokinetics, drug-likeness and medicinal chemistry friendliness of small molecules. *Scientific Reports*, *7*(1), 42717. https://doi.org/10.1038/srep42717

17- Pires, D. E., Blundell, T. L., & Ascher, D. B. (2015). pkCSM: Predicting Small-Molecule Pharmacokinetic and Toxicity Properties Using Graph-Based Signatures. *Journal of medicinal chemistry*, *58*(9), 4066–4072. https://doi.org/10.1021/acs.jmedchem.5b00104

18- IBM Corp (2022). IBM SPSS Statistics for Windows (29). versions 29, 29.0.1. https://www.ibm.com/docs/en/spss-statistics/29.0.0?topic=overview-whats-new-in-versions-29-2901

19- McHugh, M. L. (2013). The Chi-square test of independence. *Biochemia Medica*, *23*(2), 143. https://doi.org/10.11613/BM.2013.018

Creative Commons Attribution-Non-Commercial 4.0 International License

Published by DAC Democratic Arabic Center
DAC Democratic Arabic Center GmbH, Berlin

20- Hu, M., & Chua, S. L. (2025). Antibiotic-Resistant Pseudomonas aeruginosa: Current Challenges and Emerging Alternative Therapies. *Microorganisms*, *13*(4), 913. https://doi.org/10.3390/microorganisms13040913

21- Yin, C., Alam, M. Z., Fallon, J. T., & Huang, W. (2024). Advances in Development of Novel Therapeutic Strategies against Multi-Drug Resistant Pseudomonas aeruginosa. *Antibiotics*, *13*(2), 119. https://doi.org/10.3390/antibiotics13020119

22- Bertoni, M., Kiefer, F., Biasini, M., Bordoli, L., & Schwede, T. (2017). Modeling protein quaternary structure of homo- and hetero-oligomers beyond binary interactions by homology. *Scientific reports*, *7*(1), 10480. https://doi.org/10.1038/s41598-017-09654-8

23- Williams, C. J., Headd, J. J., Moriarty, N. W., Prisant, M. G., Videau, L. L., Deis, L. N., Verma, V., Keedy, D. A., Hintze, B. J., Chen, V. B., Jain, S., Lewis, S. M., Arendall, W. B., 3rd, Snoeyink, J., Adams, P. D., Lovell, S. C., Richardson, J. S., & Richardson, D. C. (2018). MolProbity: More and better reference data for improved all-atom structure validation. *Protein science : a publication of the Protein Society*, *27*(1), 293–315. https://doi.org/10.1002/pro.3330

24- Alharbi, M. S., Moursi, S. A., Alshammari, A., Aboras, R., Rakha, E., Hossain, A., Alshubrumi, S., Alnazha, K., Khaja, A. S. S., & Saleem, M. (2025). Multidrug-resistant *Pseudomonas aeruginosa*: Pathogenesis, resistance mechanisms, and novel therapeutic strategies. *Virulence*, *16*(1), 2580160. https://doi.org/10.1080/21505594.2025.2580160

25- Dash, S., Sharma, A., & Kini, S. G. (2026). MraY: An emerging therapeutic target in bacterial peptidoglycan biosynthesis for the discovery of novel antibiotics from natural and synthetic origin. *European journal of medicinal chemistry*, *301*, 118234. https://doi.org/10.1016/j.ejmech.2025.118234

26- Jimenez, D. G., Poongavanam, V., & Kihlberg, J. (2023). Macrocycles in Drug Discovery—Learning from the Past for the Future. *Journal of Medicinal Chemistry*, *66*(8), 5377. https://doi.org/10.1021/acs.jmedchem.3c00134

27- Amrhein, J. A., Knapp, S., & Hanke, T. (2021). Synthetic Opportunities and Challenges for Macrocyclic Kinase Inhibitors. *Journal of medicinal chemistry*, *64*(12), 7991–8009. https://doi.org/10.1021/acs.jmedchem.1c00217

Creative Commons Attribution-Non-Commercial 4.0 International License

Published by DAC Democratic Arabic Center
DAC Democratic Arabic Center GmbH, Berlin

28- Ríos-Rozas, S. E., Valdés-Muñoz, E., Rojas-Santander, V., Farías-Abarca, J., Hernández-Rodríguez, E. W., Contreras, H. R., Palma, J. M., Suardíaz, R., Osorio, M. I., Yáñez, O., Morales-Quintana, L., & Bustos, D. (2026). Drug Repurposing Uncovers New Chemical Scaffolds as Potent Urease Inhibitors: A Comprehensive Computational Study. *International Journal of Molecular Sciences*, *27*(8), 3561. https://doi.org/10.3390/ijms27083561

Creative Commons Attribution-Non-Commercial 4.0 International License

Published by DAC Democratic Arabic Center
DAC Democratic Arabic Center GmbH, Berlin